PREEQUILIBRIUM MODELS IN GENERAL; THE GRIFFIN MODEL IN PARTICULAR[1]

CONSTANCE KALBACH,* Saclay

This paper presents a general survey of the four most commonly used preequilibrium models for nuclear reactions: the intranuclear cascade + evaporation model, the Fermi-gas-equilibration model, the Griffin or exciton model, and finally the hybrid and geometry dependent hybrid models. These models all deal with the transition of an intermediate nucleus from an initial state with relatively few degrees of freedom to a condition of steady state equilibrium corresponding to the compound nucleus of Bohr, and all predict the energy spectra of the emitted particles. The basic features common to these preequilibrium models are presented and a comparison is made of the basic assumptions, the methods of calculation, and the special advantages and disadvantages of the various models. It is shown that the optimum model to use in a given situation depends on the system being studied and the information desired as well as on the personal tastes of the user. In the second part of this paper, the Griffin model, which is the one most frequently used to study neutron induced reactions, is examined in more detail. The description it provides of the nuclear equilibration process is summarized, and the evaluation and physical significance of the effective empirical values for the model parameters n_0 and M^2 are discussed. Finally, the effects of isospin conservation and of the pairing interaction are considered. These phenomena represent open problems for the preequilibrium model and are examples of how the model can be used to arrive at new physics.

I. INTRODUCTION

For many years it has been customary to divide nuclear reactions into two extreme categories. First there are the very fast, direct reactions which occur on a time scale comparable to the time necessary for the projectile to traverse a nuclear diameter. These reactions are usually treated by microscopic means. At the other extreme we have the compound nucleus reactions which occur on a very much longer time scale and are treated by statistical means. The past 6 to 8 years, however, have seen the growth of a number of nuclear reaction models designed to „bridge the gap" and to present a more unified picture of nuclear reactions. Thus these preequilibrium models must attempt to describe, usually in statistical terms, the intermediate phases of a reaction which occur between the first target-projectile interaction and the attainment of the steady state equilibrium which characterizes the compound nucleus.* In these models and in the discussion presented here, we restrict ourselves generally to systems with 20 to 100 MeV of excitation in the intermediate or composite nucleus and with the mass numbers of or higher.

Section II of this paper presents a general discussion of preequilibrium models: the kinds of processes they try to explain, their common features, their differences, and their relative regions of applicability. Section III presents a closer look at one of the most useful and most used models for studying neutron induced reactions. This is the model first proposed by Griffin [1]. Section IV discusses some open problems in the field of preequilibrium reactions. It tries to demonstrate that we are now in a position where the models can shed new light on physics while physics is showing us where to improve the models.

II. PREEQUILIBRIUM MODELS IN GENERAL

II. 1. Processes to be described

Figure 1 shows a schematic picture of a nuclear reaction. The width of the „tree" represents the reaction cross section, while the vertical axis shows the number of collisions made by the projectile inside the nucleus. It is essentially a time axis. In the zero collision limit, we have elastic scattering by the nuclear potential. If particles are emitted after the first collision, we have the familiar direct reaction. Emission after two collisions might be termed a semi-direct reaction. As more and more interactions occur inside the nucleus, the energy brought into the system by the projectile gets divided among more and more particles, and the probability that one particle will have enough energy to escape the nucleus decreases. After a sufficiently large number of collisions, the energy of the system becomes completely randomized and we have a stationary state configuration (except for the continuing emission of particles). This is the familiar compound nucleus which has a fairly low particle emission rate.

[1] Lecture given at the International Symposium on Neutron Induced Reactions, September 2—6, 1974 at SMOLENICE, Czechoslovakia.

* Département de Physique Nucléaire/Basse Energie, CEN SACLAY, France.

* The term „compound nucleus" is used here to refer only to an intermediate nucleus at statistical equilibrium. The same system before equilibrium is reached is called the „composite nucleus".

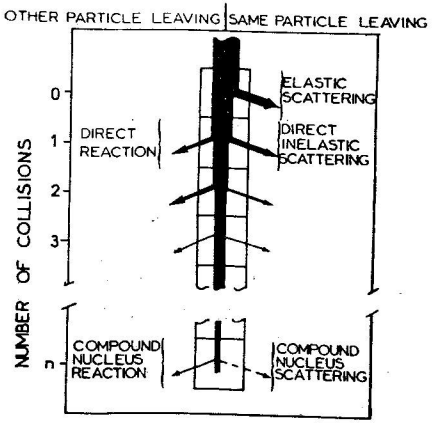

Fig. 1. Schematic picture of the course of a medium energy nuclear reaction.

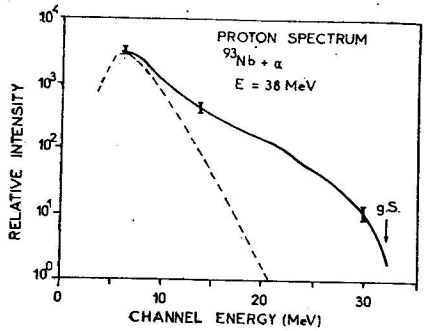

Fig. 2. Schematic illustration of data to be reproduced by preequilibrium models. The heavy line shows the experimental data [2] while the dashed curve shows the evaporation or compound nucleus contribution. The arrow indicates the energy of the ground state transition.

We know that experimentally we see the direct reactions because of the high emission probability after the first interaction and the compound nucleus processes because of the relatively long lifetime of the equilibrium configuration. But how important are the other intermediate processes? Figure 2 shows an angle intergated proton spectrum obtained with 40 MeV α-particles incident on a ^{93}Nb target [2]. The dashed curve shows the amount of the cross section which can be accounted for by compound nucleus model calculations. The arrow indicates the energy of the ground state transition, and a direct reaction model should be able to account for the cross section to discrete bound states in the final nucleus. These results, if suitably averaged in energy, might account for the upper 5 MeV or so of the spectrum. But how much of the intermediate region represents direct cross section and how much is due to intermediate processes? The preequilibrium models attempt to answer such questions and to account for energy spectra such as the one in Fig. 2 in their entirety.

II. 2. Common features of the models

There are basically four models which have been used in this type of analysis and which are considered here. They have been collected into a zoological park which is shown in Fig. 3. The first animal in the zoo was a gift from the high energy zoological park. It is the intranuclear cascade model which has

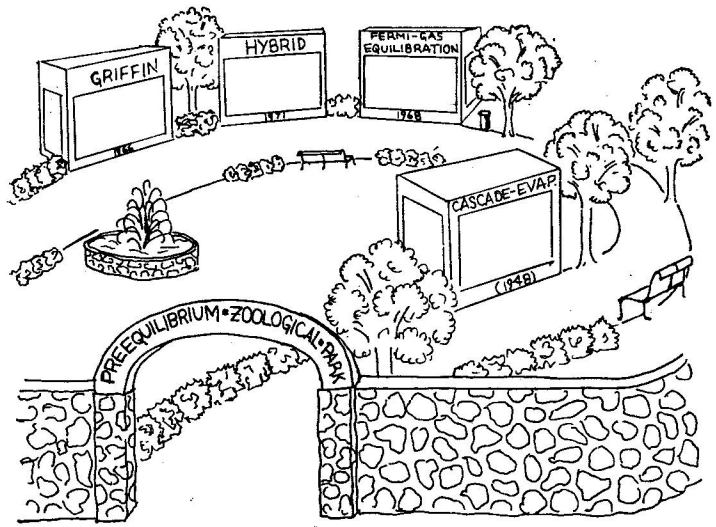

Fig. 3. Schematic representation of the current collection of preequilibrium reaction models.

proved to be fairly useful even at bombarding energies as low as 14 MeV. The other three models are much younger and are found only here in medium energy preequilibrium reactions. They are also similar in that they all rely on phase space arguments as part of their diet.

All four models have several things in common. The initial projectile energy is assumed to be redistributed through a series of energy-conserving two-body interactions leading to the creation of new degrees of freedom. They are all statistical. They do not take nuclear structure or angular momentum effects into account and cannot reproduce transitions to specific final states. Their main utility is in calculating total (angle integrated) energy spectra for emitted particles or total excitation functions for the production of a given product species.

The individual models are classified here according to the degree to which they are either realistic or phenomenological. In realistic models we hope that the approximations made are valid, and we take as much of the input as possible from the results of other types of experiments. In phenomenological models we admit that the approximations may not always be valid, but we hope that their failure can be compensated for by using effective empirical values for the model parameters. All we expect is that these parameter values should show a systematic variation from one system to another. In classifying the models, it is also useful to remember that there are basically

two parts to a preequilibrium calculation. The first is the description of the series of two-body interactions which brings the system to its equilibrium or compound nucleus configuration. The second is the calculation of particle emission during this equilibration process. These may or may not be handled in the same way in a given model. The basic features of the four models to be discussed are summarized in Table 1 which lists them roughly in order, starting with the most detailed and proceeding to the simplest.

II. 3. The intranuclear cascade + evaporation model

The cascade model [3] is shown schematically in Fig. 4 [4]. The projectile, in this case a proton, enters the nucleus at an impact parameter b. It travels a certain distance, strikes a target nucleon and exites it. The scattered nucleons then each travel through the nucleus striking and scattering other nucleons. At each collision site, three things may occur: (1) the incident and struck nucleons may both scatter with significant amounts of energy (2) one or both may have an energy below some minimum cut-off energy, in which case they are not followed any further, or (3) the collision may be forbidden by the Pauli exclusion principle. The trajectory of an excited particle is followed until it either crosses the nuclear surface and escapes or its energy falls below the cut-off value. When all particles of a given cascade have been followed, the total energy left in the residual nucleus, the identity of this nucleus and the energies and angles of all emitted particles are stored. A new impact parameter is chosen, and a new cascade is calculated. This process is repeated until a statistical number of events has been calculated. The excited residual nuclei are then used as the starting point for evaporation calculations which describe the compound nucleus part of the reaction.

The basic features of this model are shown in the first line of Table 1. It is a realistic model, using free nucleon-nucleon scattering cross section data and a fairly physical nuclear density distribution. In calculating both the

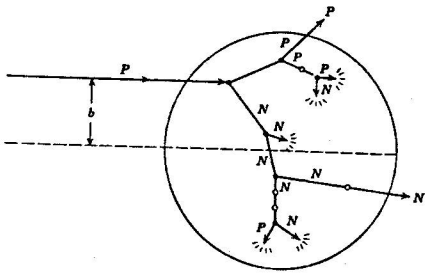

Fig. 4. Schematic picture of the intranuclear cascade + evaporation model showing the trajectories of excited particles. Open circles represent collisions which are forbidden by the Pauli exclusion principle. Short arrows ending in a series of little lines correspond to particles with energies below a present cut-off energy (from [4]).

Table 1

Basic features of current preequilibrium models

Model	Type	Bookkeeping		Method	Special Calc.
		Equil.	Emiss.		
Cascade + Evap. (1945)	realistic geometry	positions energies momenta	positions energies momenta	Monte-Carlo	angular distrib.
Fermi-Gas-Equil. (1968)	realistic phase space	energies	energies	master equation	
Hybrid (and *GDH*) (1971)	phenomenological phase space	number	energies	closed form	complex particles in
Griffin (or Exciton) (1968)	phenomenological phase space	number	number	master equation	complex particles in and out

nuclear equilibration and particle emission, it considers the position, energies and momenta of the excited particles. It is thus the most detailed of the models and has the advantage that it can calculate angular distributions for the emitted particles as well as their total energy spectra.

II. 4. The Fermi-gas-equilibration model

The Fermi-gas-equilibration model [5, 6] is shown schematically in Fig. 5. The single states of the nucleus are taken to be those of a Fermi gas. These states are then classified into different groups according to their energy, and the model considers, at each stage of the reaction the probability p_i that an average state in the i-th group is occupied. The reaction starts with all of the low energy states filled (corresponding to the target nucleus in its ground state) and with one nucleon (the projectile) in a highly excited state. This gives the group occupation probabilities at the time zero which are shown in the figure. Two-body interactions then lead to the redistribution of the strength until a steady state condition is reached. At each time during the equilibration process, the energy spectrum of emitted nucleons can be calculated and a net spectrum obtained.

The basic features of the model are given in the second line of Table 1. Like the cascade model, it is also realistic, taking its input from free nucleon-

-nucleon scattering cross sections, but the Fermi-gas-equilibration model considers only the energies of the excited particles. All geometrical information is ignored. The calculations are performed using a rather large set of coupled equations, and, of course, no angular distributions can be obtained since neither angular momentum conservation nor the reaction geometry is considered. This is, in fact, true of all the remaining models. The Fermi-gas-equilibration model does, however, provide a unified description of the reaction process, with a smooth and natural transition between the preequilibrium and equilibrium phases.

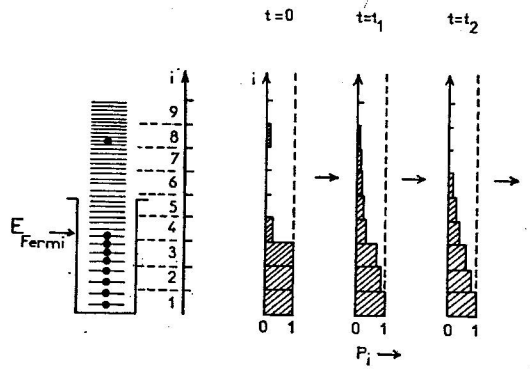

Fig. 5. Schematic representation of the Fermi-gas-equilibration model. The set of single particle states is shown on the left. On the right, the shaded areas correspond to the occupation probabilities for each group of single particle states. Succesive drawings represent later and later times during equilibration.

II. 5. The Griffin or exciton model

At this point it is advantageous to consider the Griffin or exciton model and return later to the hybrid model which is a cross between this and the Fermi-gas-equilibration model. The Griffin model [1, 7—13] is the simplest of those in the Table and is pictured in Fig. 6. The nuclear potential is shown with a set of equally spaced single particle states. The projectile enters, forms a $1p-0h$ (or 1 exciton) state and then interacts with one of the target nucleons to form a $2p-1h$ (or 3 exciton) state.* Further interactions create more and more particle-hole pairs. Eventually, when there are enough particles and holes, pair annihilation will start to drive the process backward, and again

* The term exciton refers collectively to excited particle and excited hole degrees of freedom.

a steady state condition is achieved. Thus, in essence, this is much like the previous model except that it is less detailed. The states of the system are classified only according to the number of particles *and* hole degrees of freedom which they contain, and the equilibration process is followed by calculating the occupation probabilities for different groups of nuclear states rather than different groups of single particle states. In each group of nuclear states there will be some unbound states which can undergo particle emission. These are shown in the upper part of the figure. We can calculate the average rate for particle emission for each class of states and combine these with the occupation probabilities to obtain preequilibrium emission spectra.

The basic properties of the model are shown in the fourth line of Table 1. The Griffin model is phenomenological. It is much simpler than the others we have considered and, therefore, uses effective empirical parameter values. As already mentioned, the model considers only the number of excited particles

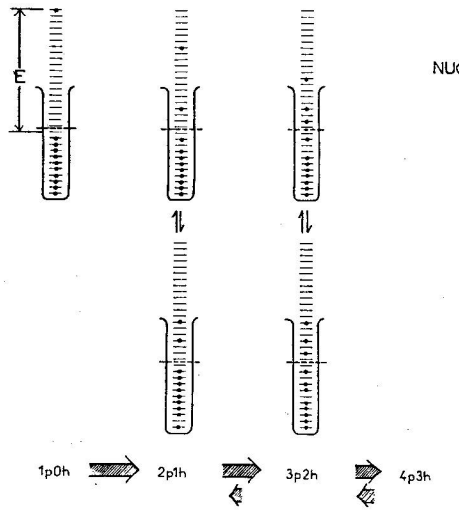

Fig. 6. Schematic representation of the first stages of a reaction in the Griffin model. The horizontal lines indicate the equally spaced single particle states in the potential well. The number of excited particle and hole degrees of freedom is listed for each configuration.

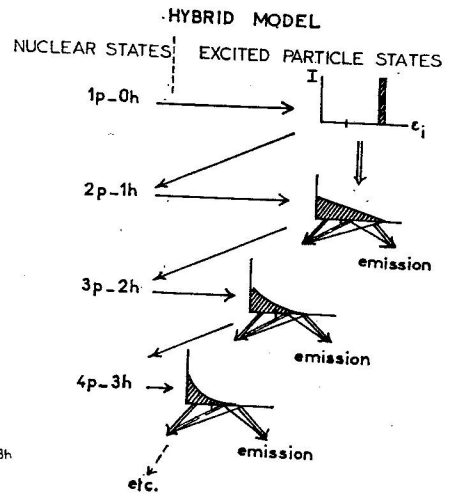

Fig. 7. Schematic representation of the first few stages of a reaction in the hybrid model. The small graphs show the energy distribution of the excited particle in each class of states. The arrows between them represent relative transition probabilities for particle emission and particle-hole pair creation. The zero of the energy scale is the Fermi energy and the mark on the axis indicates the emission threshold.

and holes, both in following the equilibration process and in calculating particle emission. Like the Fermi-gas-equilibration model, it uses a set of coupled equations to follow the equilibration process, but these equations are much simpler and faster to solve. By giving up detailed information about the nucleus, the model has the ability to treat a greater variety of reactions. In particular, it has the advantage of being able to perform calculations for reactions involving complex particles (d, t, α) as projectiles and of calculating emission spectra for such particles as well.

II. 6. The hybrid model

Finally let us look at the hybrid model [14, 15] which is so named because it attempts to combine essential features of both the Fermi-gas-equilibration and the Griffin models. It is shown schematically in Fig. 7. We again start with a set of equally spaced single particle states and, as in the Griffin model, we classify the states of the nucleus according to the number of excited particles and holes they contain. Once again an incident nucleon can be thought of as forming a $1p-0h$ state with the target nucleus and then interacting with a target nucleon to form a $2p-1h$ state. Again additional two-body interactions are assumed to lead to the creation of more particle-hole pairs. But now, for each class of nuclear states, the exitation energy distribution for the excited particles is calculated. The small graphs in the Figure show the relative probabilities of finding an excited particle in a single particle state of a given energy, ε_i, above the Fermi energy. For each particle excitation energy, the branching ratio for particle emission relative to the creation of an additional particle-hole pair is calculated, much as is done in the Fermi-gas-equilibration model. Starting with the initial $2p-1h$ configuration, one considers each set of states in turn. All of the strength which goes into particle emission contributes to the preequilibrium spectrum, while all of the strength which goes into pair creation is assumed to be randomly distributed among all states of the next degree of complexity. This process is repeated until the most probable exciton number in the equilibrium system is reached or until all of the cross section has already gone into particle emission. One then proceeds to a standard compound nucleus model calculation for the equilibrium part of the reaction.

The basic features of this model are shown in line 3 of Table 1. It is a blend of a phenomenological and a realistic one and is what I would call „phenomenolistic". In following nuclear equilibration, it considers only the number of excited particles and holes. In calculating particle emission rates, on the other hand, it considers the excitation energies of the individual particles.

It performs only closed form calculations. This saves a little on computer time relative to the Griffin model, but also sacrifices a little on accuracy and, as in the cascade model, there remains here an artifical division between the preequilibrium and equilibrium parts of the reaction. Like the Griffin model, the hybrid model can treat complex particles as projectiles, but since particle emission is handled as in the Fermi-gas-equilibration model, it has been possible to calculate only the emission of nucleons. This question is discussed in the contribution of Obložinský.

There is a refinement to the hybrid model which is called the geometry dependent hybrid (or *GDH*) model [16, 17] and in which some of the nuclear geometry effects which are considered in the cascade model are introduced. In particular, the inclusion of regions of reduced nucleon density (and thus also reduced well depth) seems to lead to an improved agreement with the experiment when compared with the normal hybrid model calculations. Thus it seems that when the phenomenological approach is abandoned, the data demand that more and more realistic details be included.

II. 7. Comparison between models

These then are the models which live in our zoo. Figure 8 shows comparisons of predictions of all the models with the experimental data. Since in this type of work an agreement to within a factor of two is considered reasonable, I feel that it is difficult to choose between the models on the basis of such comparisons. In addition it is interesting to note the difference between the two cascade model calculations for ^{181}Ta + p. These were obtained with the Oak Ridge (upper) and Columbia-Brookhaven (lower) computer codes which are compared in Ref. [3].

Which then is the best, the most interesting, the most useful model? The answer depends partly on personal taste and very much on the kind of data to be considered. The phenomenological vs. realistic model choice is largely one of aesthetics. Realistic models can be said to contain more physics, and this is possibly true. Also it is somehow satisfying to start with fundamental nucleon-nucleon scattering cross sections and a nuclear density distribution and to calculate what happens in a nuclear reaction. But phenomenological calculations are often far simpler and with a wider range of applicability; and there is interesting physics which may emerge from the effective parameter values. Then there is the question of the data to be considered. If you are interested in angular distributions, you are limited to the cascade model. If you are interested in deuteron or alpha particle spectra, you are limited to the Griffin model.

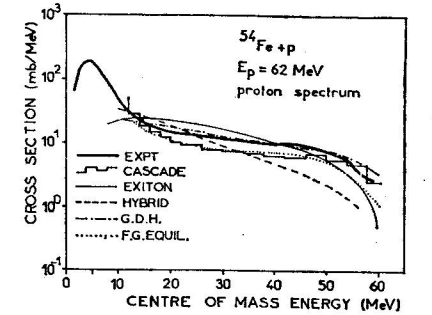

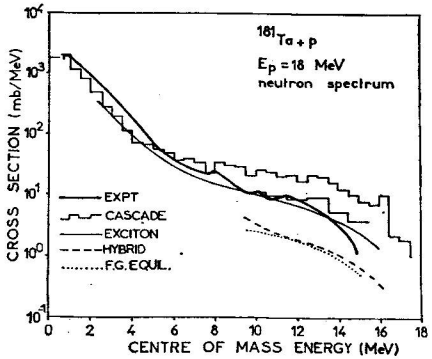

Fig. 8. Comparison between experimental angle-integrated nucleon spectra and the calculated spectra from various preequilibrium models. Evaporation components are shown included in only some of the calculated results. References: experiment (*a*) = Ref. [18], (*b*) = Ref. [19]; cascade (*a*) = Ref. [18], (*b*) = Ref. [19] (upper) and [6] (lower); exciton (*a*) and (*b*) = present work; hybrid (*a*) = Ref. [16], (*b*) = Ref. [15]; *GDH* (*a*) = Ref. [16]; F.–g. equilibration (*a*) = Ref. [20], (*b*) = Ref. [6].

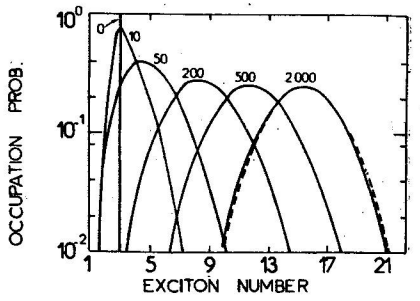

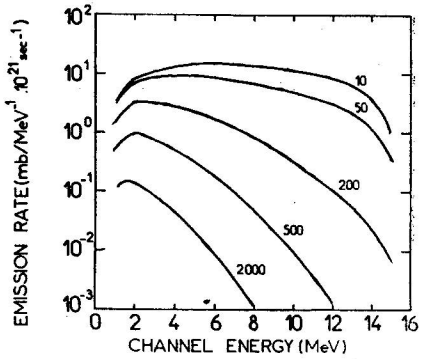

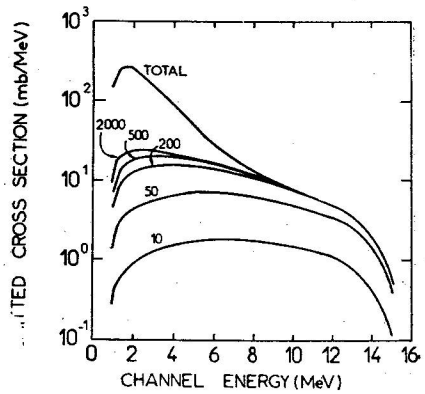

Fig. 9. Results of coupled channel calculations for a system with $A = 100$ and 24 MeV of excitation. The numbers next to the curves indicate the number of elapsed time increments. The dashed curve corresponds to the equilibrium limit of the occupation probabilities. One time increment is equal to about 10^{-23} sec.

III. THE EXTENDED GRIFFIN MODEL

I would like now to display some of my own preferences and to concentrate on the simplest of the models, the exciton or extended Griffin model. As we have seen, it is a phenomenological model in which the states of the system are classified according to the number of excited particles and holes they contain. It follows the evolution of the composite nucleus towards equilibrium as a function of time by solving a set of coupled equations on a computer. Let us now look first at how the model describes the nuclear equilibration process, then at the empirical values for the model parameters as found from data analyses, and finally at its utility in describing data when systematic values for the parameters are chosen.

III. 1. Nuclear equilibration

The coupled master equations [10] which are solved have the form

$$\frac{\mathrm{d}P(n,t)}{\mathrm{d}t} = P(n-2,t)\lambda_+(n-2) + P(n+2,t)\lambda_-(n+2) -$$

$$- P(n,t)[\lambda_+(n) + \lambda_-(n) + \sum_\nu \int \lambda_\nu(n,\varepsilon)\,\mathrm{d}\varepsilon];$$

where $P(n, t)$ is the probability of finding the system in a state with n excitons at the time t. Here n is used to denote the two variables p and h which are coupled by the fact that particles and holes are created and destroyed together in pairs. The quantities λ_+ and λ_- are average particle-hole pair creation and destruction rates derived from time dependent perturbation theory, and $\lambda_\nu(n, \varepsilon)$ is the average rate for emitting particles of type ν and energy ε from an n-exciton state. It is derived from microscopic reversibility. Thus we have a set of flow equations where the first line represents the strength gained by the n-exciton states in the time $\mathrm{d}t$ and the second line represents the strength lost.

The results obtained from solving these equations are shown in Fig. 9. The occupation probabilities in the upper part of the figure are shown as a function of the exciton number for various numbers of the elapsed time increments in the computer. Initially, all the strength is assumed to start in a $2p-1h$ state. As equilibrium proceeds, the most probable exciton number gets larger. The changes are most rapid in the early stages of the reaction when the system is far from equilibrium and are very slow as equilibrium is approached. A steady state solution is reached after about 2000 iterations, and this solution corresponds to the equilibrium configuration predicted by

the postulate of equal probabilities for all nuclear states and shown as a dashed curve. Thus there is internal consistency in the model.

The middle part of Fig. 9 shows the behaviour of the instantaneous neutron emission spectra. The emission rate is shown as a function of the neutron energy, again for various numbers of the elapsed time increments. Initially, the emission rate is relatively high and the spectrum is essentially flat. As the available energy gets divided among more degrees of freedom, the emission rate decreases and decreases most rapidly for the high energy particles. At equilibrium, an evaporation like spectrum is observed, and the emission rate is about a factor of 100 lower than at the beginning of the reaction. Again the picture given by the model is physically reasonable.

The lower part of Fig. 9 shows the total spectrum of particles emitted during the indicated number of time increments. We find that most of the preequilibrium component (the part emitted in 2000 time increments) is emitted very early in the reaction while during the last 3/4 of the equilibration time the total spectrum changes very little. The curve labelled „total" shows the spectrum when the full reaction cross section has been exhausted. The particle emission rate at the attainment of equilibrium would correspond to a mean compound nucleus lifetime of the order of 1.5×10^{-18} sec while the equilibration time is, within the same model framework, about 2.0×10^{-20} sec or two orders of magnitude smaller, and most of the preequilibrium cross section is emitted in the first 10^{-21} sec or so. Thus we see here that the reaction divides naturally into two parts: a fast preequilibrium part dominated by particles emitted very early in the reaction, and a compound nucleus part which grows in over a very much longer time scale. This begins to look again like the direct + compound nucleus picture we are trying to get away from, but in the present formalism the fast component of the reaction includes everything which has been neglected before.

III. 2. Effective parameter values

There are basically three parameters in the extended Griffin model. The first is the density, g, of equally spaced single particle states. This enters into the calculations of the total state densities for a given particle-hole configuration (needed in calculating particle emission rates) and of the density of final states accessible in a particle-hole pair creation or destruction interaction. The second parameter is the number of degrees of freedom, $n_0 = p_0 + h_0$, in the initial system and determines the starting point for the integration of the flow equations. Finally, the third parameter is the square of the average matrix element for the residual interactions leading to pair creation and destruction.

The density of single particle states has generally been treated in a realistic way. That is, it has not been treated as a free parameter. Values obtained from the analysis of level density experiments and compound nucleus reactions have been used. The tabulated values of Gilbert and Cameron [21] which take some account of shell structure are often used, as is the simple prescription $g = (A/13)\,\mathrm{MeV}^{-1}$, which ignores shell effects and leaves them to be considered as a separate question. This latter prescription is adopted here. This leaves two parameters which were, in the first model analyses, treated as adjustable.

Figure 10 shows the results for the initial configuration obtained from analyzing the shapes of the energy spectra for emitted particles. The lower graph is for nucleon induced reactions and the points are seen to cluster around a value of $n_0 = 3$, presumeably corresponding to a $2p-1h$ configuration. An initial $1p-0h$ state would lead only back into the elastic channel and would not be observed in the analysis. The upper graph is for α-particle induced reactions and shows results clustering between values of $n_0 = 4$ and $n_0 = 5$. Four excitons could correspond to a $4p-0h$ state formed by the α-particle „dissolving" in the nuclear potential. It would thus be analogous to the $1p-0h$ state for incident nucleons. There are a number of points in Fig. 10 which show significantly larger n_0 values, and these are seen to fall either in the lead or tin mass regions. They are fairly well understood in terms of shell structure effects on the residual nucleus state densities, and correspond to the only systems among those included in the figure which are predicted to show shell effects in the form of unusually high effective n_0 values. On the basis of these results, initial configurations of $2p-1h$ (nucleon induced reactions) or $4p-0h$ (α-particle induced reactions) are often assumed in performing model calculations, and are consistent with our physical intuition as well as with data analyses.

Figure 11 shows how the importance of preequilibrium emission varies with excitation energy. The quantity plotted is the fraction of the reaction cross section which involves preequilibrium emission of at least one particle. As would be expected, this quantity increases with increasing excitation energy. From results such as these, effective residual two-body matrix elements can be estimated [22]. The squares of the matrix elements show the mass and excitation energy dependence predicted by the results of nuclear matter calculations and have a normalization which is projectile dependent

$$M^2 = K_a A^{-3} E^{-1}.$$

When the corrected rate expressions of Ribansky et al. [12] are used, the values of K_a are 190 MeV^3 and 1450 MeV^3 (±30 %) for proton and α-particle induced reactions, respectively. The resulting transition rates are in reasonable

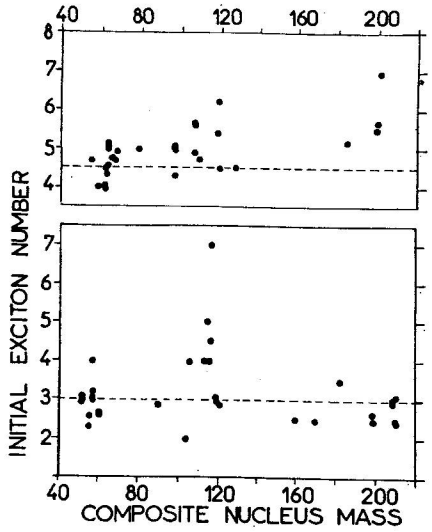

Fig. 10. Summary of the initial exciton numbers found from data analysis. The upper graph is for α-particle induced reactions and the lower graph is for nucleon induced reactions. The dashed lines show the average trend of the results.

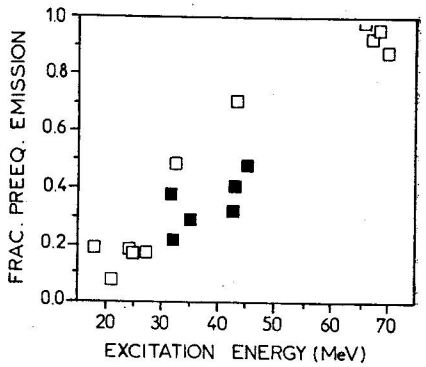

Fig. 11. Summary of values for the fraction of preequilibrium emission obtained from data analysis. Open and solid points are for nucleon and α-particle induced reactions, respectively.

agreement with the results [23] on neutron induced reactions at lower energies and on fairly heavy targets. However, it should be emphasized that while the general magnitude of K_a is significant, the exact numerical values depend critically on such factors as the value of the single particle state density used, the way in which proton-neutron distinguishability is taken into account, and the way in which the initial excitons are divided into particles and holes.

III. 3. Comparison with data

With the parameter values summarized in Sect. III. 2. we are now in a position to calculate emission spectra with no adjustable parameters. Two such spectra were compared with angle integrated data in Fig. 8. Several more will be presented in Sect. IV. Here I want simply to show one example for complex particle spectra. Figure 12 shows a comparison of calculation and experiment for reactions induced on ^{54}Fe by 29 and 62 MeV protons.

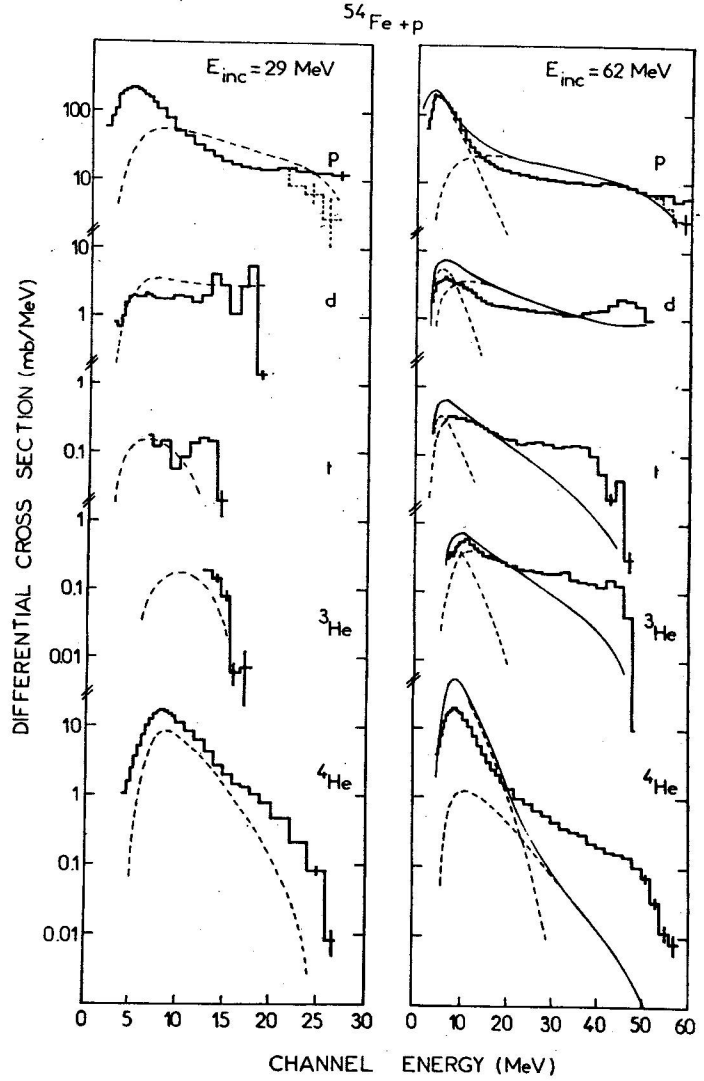

Fig. 12. Comparison between calculation and experiment for angle integrated charged particle spectra in reactions induced by 29 and 62 MeV protons on ^{54}Fe. The bar graphs show the data, the solid curves are the full calculated spectra and the dashed curves show the preequilibrium (high emission energy) and equilibrium (low emission energy) components. Only the preequilibrium component is shown for the 29 MeV incident protons.

The fits to the proton and deuteron spectra are good, while for the tritons, ^{3}He and ^{4}He, noteably at 62 MeV, there are high energy particles which are unaccounted for in the calculations. Both the spectral shapes for these particles and the fact that their number increases with increasing bombarding energy are consistent with a direct, one-step pickup mechanism [10]. Since this would involve 3- and 4-body interactions, such direct reactions cannot be calculated in the model. These same particles have also been considered [24] by counting the number of ways that the final emitted cluster energy (binding plus kinetic) may be divided among the constituent nucleons while they are still inside the nucleus. This improves agreement with the data but has certain difficulties in its formal justification. The significant point in Fig. 12, however, is not the disagreement but rather the level of accord between calculation and experiment. The equilibrium components shown indicate how little of the observed cross section can be accounted for in a compound nucleus calculation and how much of an improvement is provided by the Griffin model, particularly at the lower bombarding energies.

The extended Griffin model still ignores nuclear geometry effects; and angular momentum effects have been investigated [13], but not yet included in the full master equation calculations. Similarly shell effects are understood, but are still in the process of being included in the full model. The role of pairing forces is discussed in Sect. IV. None of these things, however, seems to prevent the model from being extremely useful in describing a wide variety of reaction systems; and as long as one is not right at a major shell closure, calculations can be performed fairly simply with no adjustable parameters. The combination of simplicity and utility is what makes the Griffin model my favourite animal in the preequilibrium zoo.

IV. CURRENT PROBLEMS AND REGIONS OF INVESTIGATION

Now that we are hopefully convinced that the Griffin model can reproduce the general features of particle spectra, we can start to look at second order effects in the model and to try to gain some information about nuclear structure. Regions of current active investigation within the Griffin model framework include the angular momentum, pairing and shell structure effects, the possible influence of α-cluster structures on direct (n, α) and (p, α) reactions, and the problem of isospin conservation. In the present report it is possible to cover only two of these; the pairing and isospin effects. Both of these fields are ones in which the study of neutron induced reactions will be very important in understanding the physics.

IV. 1. Isospin conservation

The general system of levels for nuclei with a neutron excess is shown schematically in Fig. 13. The lowest lying states will have the lowest possible isospin (i.e. equal to its z-component). At some higher excitation energy, a set of states with one additional unit of isospin, the $T_>$ states, will begin. Both sets of states will increase exponentially in density with the excitation energy, but since the $T_>$ states begin at a higher energy, they will always be far less numerous than the $T_<$ or ground state isospin states.

In proton (or ^{3}He) induced reactions on targets with the isospin T_0, a fraction $1/(2T_0 + 1)$ of the composite nucleus formation cross section, forms

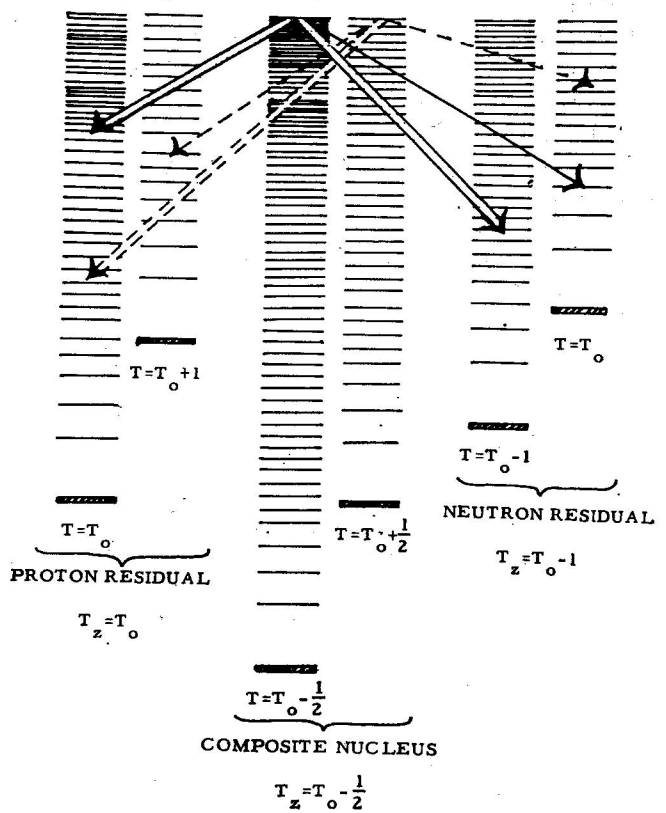

Fig. 13. Schematic drawing of the role of isospin selection rules in nuclear decay. The relative thicknesses of the arrows represent the relative decay probabilities for the states of a given isospin.

states in the intermediate nucleus with the isospin $T = T_>$, while the remaining (and usually major) fraction of the cross section, $2T_0/(2T_0 + 1)$, goes into the more abundant $T_<$ states. In neutron and α-particle induced reactions only composite states of the ground state isospin are populated. The question then is: „Two what extent is isospin conserved as a good quantum number?"

If the isospin is mixed and all composite states are populated with an equal probability, the decay observed will be essentially characteristic of the very much more aboundant $T_<$ states. Thus the decay pattern for a proton induced reaction will look like that for a neutron induced reaction with dominant branches for both neutron and proton emission. If isospin is conserved, there is a chance to observe the $T_>$ state decay. For the $T_>$ states, the neutron emission is blocked or hindered because the residual states of the lowest isospin are forbidden. The proton channel carriers essentially all of the strength and the proton yield is enhanced.

Experimental results both in the nickel region [24—29] and for nuclei with $A \gtrsim 100$ [30, 31] have indicated that for proton induced reactions with about 20 MeV of excitation energy in the composite nucleus, isospin is conserved as a quantum number in at least 40—80 % of the decays. Since at such excitation energies, preequilibrium model calculations are often used to analyze the high energy emitted particles, one is led to the consideration of the isospin as a quantum number within the framework of the extended Griffin (or exciton) model.

So far such considerations have been limited to performing two calculations for each reaction, one each for the $T_<$ and the $T_>$ composite states, assuming complete isospin conservation. The method of including the isospin as a quantum number is analogous to that employed in equilibrium models. In particular, the $T_<$ state densities are approximated by the total state densities, while the state densities for the $T_>$ states have the same functional form but use an excitation energy calculated relative to the energy of the lowest level of this isospin. The model parameters g, p_0, h_0, and M^2 are assumed to have the same values for both isospins.

Figure 14 [30] shows the resulting description of the instantaneous proton spectra during the equilibration process. For both of the composite isospins, the proton spectra start out, being abundant in high energy particles and show the usual transition to an evaporation like shape. For the $T_<$ states the usual rapid decrease in the emission rate is also observed; while for the $T_>$ states, the emission rate for low energy particles increases initially as more complex states are populated. The decrease in the emission rate later in the reaction occurs because most of the $T_>$ cross section has already gone into particle emission. Thus while most of the $T_<$ cross section (87 % in this

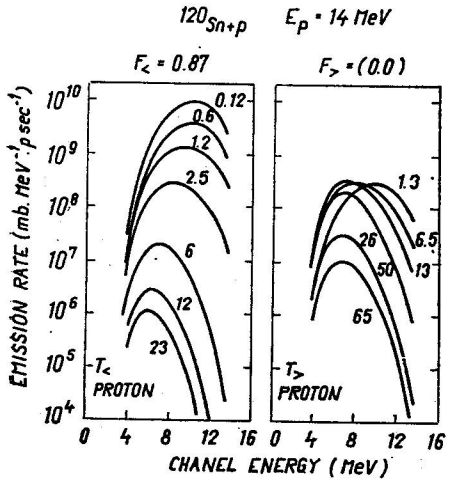

Fig. 14. Comparison of the instantaneous proton emission rates for the $T_<$ and $T_>$ states of a ^{121}Sb composite nucleus assuming complete isospin conservation. The numbers next to the curves indicate the elapsed time in units of 10^{-21} sec. The values for the fraction of the cross section left at equilibrium are also indicated (form [30]).

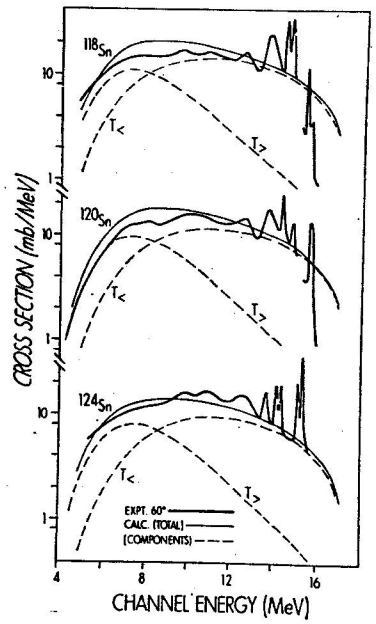

Fig. 15. Comparison of calculated and experimental Sn(p, p') spectra. The calculated component spectra are for preequilibrium decay. The $T_<$ equilibrium strength goes into the neutron channel (form [30]).

example) involves equilibrium particle emission, essentially none of the $T_>$ cross section survives the equilibration process. The predicted difference in behaviour between the emission rates for the two isospins is a consequence of phase space considerations and is not physically unreasonable. However, the prediction of an essentially completely preequilibrium decay for the higher isospin states casts some doubt on existing calculations of their level widths in an equilibrium or compound nucleus framework, and the calculated proton emission rates raise serious questions about the validity of one of the basic statistical assumptions used in the calculations.

The key statistical assumption is that of „equal a priori probabilities". In the case of a compound nucleus, it is assumed that the system is equally likely to be found in any of the nuclear states with the correct set of quantum numbers; while in the Griffin and the hybrid model calculations it is assumed only that any state with a given number of particles and holes is as likely

to be populated as any other. This assumption is the basis for calculating particle emission rates in either model. For it to remain valid one must assume that the internal transitions are fast enough to maintain the population of the unbound states since the strength from these states will be lost in the particle emission process.

The question of the relative rates for internal transitions and for particle emission has been investigated [30] for the Griffin model. It has been found that the statistical approximation is predicted to be satisfactory for both composite isospins in the early stages of the reaction. For the low isospin states it gets better, while for the high isospin states it gets worse as equilibrium is approached and cannot be considered valid in the later stages. This casts serious doubt on the validity of all existing statistical model calculations, equilibrium or preequilibrium, for the higher isospin states.

It is, of course, possible that the method of including the isospin in the Griffin model is incorrect and has led to a false conclusion. It is also possible that the statistical assumption is not valid, as predicted, but that the calculated spectra are not very sensitive to this fact. In fact, the preequilibrium model predictions are quite successful in reproducing experimental spectra, as shown in Fig. 15. However, since the $T_>$ preequilibrium component is dominated by low energy particles, almost as good a fit can be obtained with the old assumption of equilibrium decay for the high isospin states, and no conclusions can be drawn. If we had more confidence in the low energy part of the $T_<$ preequilibrium component, we might be able to extract an experimental $T_>$ spectrum, and it is here that neutron induced reactions, which populate only one composite isospin, may be helpful.

A few years ago it was assumed that the $T_>$ state decay was largely an equilibrium process and that the compound nucleus model could be used for estimating such quantities as level widths. Preequilibrium studies have shown us our own ignorance and have raised serious questions about both the reaction mechanism and the validity of one of the basic statistical postulates. We must now seek answers to these questions.

IV. 2. Pairing forces and the initial phase of the reaction

Nuclear physicists have been aware [1, 32—37] since the earliest days of the Griffin model that pairing effects might play a role in determining preequilibrium spectral shapes. First there have been investigations in which pairing effects have been included as is done in compound nucleus calculations [32—36]. A pairing enegy, δ, is subtracted from the excitation energies of the composite and residual nuclei. It is given by

$$\delta = \delta_n(N) + \delta_p(\mathrm{Z}),$$

where δ_n (or δ_p) is zero if N (or Z) is odd. This technique is only applicable for $E > \delta$, while preequilibrium calculations attempt to produce average spectra down essentially to the ground state transition. Thus, particularly for lighter nuclei where the pairing corrections are large, the utility of the approach was not clear.

Another and related question is whether the initial configuration in the composite nucleus depends on the even-odd character of the target. It was originally anticipated [1] that an unpaired nucleon in the target would be preferentially excited in the initial interaction of the projectile. Evidence obtained from data analyses remains, I believe, inconclusive. The trends observed have never been outside experimental and calculational uncertain — ties, but, on the other hand, they have not been completely explained by the simple substraction of the appropriate pairing energies.

It seems that the two possible effects of the pairing forces, a shift in the energy used in calculating state densities and a change in the initial particle-hole configuration of the composite nucleus, must be investigated simultaneously, since they can both alter the shape of the high energy portion of the emitted particle energy spectra. One way to do this is to perform a simultaneous analysis of the proton and neutron spectra from a single reaction system. If the systems are chosen so that both the proton and neutron residual nuclei are odd-A, then an energy shift should have little effect on the proton-to-neutron yield ratio while the excitation of the unpaired target nucleon would enhance the relative yield for that type of particle.

Investigations of this kind have been undertaken [31]. The initial studies have involved reactions induced by 18 MeV protons on the odd proton targets ^{103}Rh, ^{159}Tb, and ^{169}Tm. In addition, neutron spectra have been measured for the odd neutron target ^{105}Pd. All the targets have the advantage of being far from shell closures so that the influence of shell structure will be minimized.

Figure 16 shows the experimental angle-integrated proton and neutron energy spectra and the calculated results obtained using the usual $2p - 1h$ initial configuration. Complete isospin conservation was assumed and, for the right hand curves, the appropriate pairing energies were subtracted from all the excitation energies. The latter procedure produced slightly improved agreement with the data. Except for the ^{103}Rh + p system, the agreement is found to be reasonable; that is within about a factor of two. There is, however, a noticeable trend for the calculations to overestimate the high energy neutron yield while underestimating the corresponding proton yield. This effect is less pronounced for the heavier systems.

In considering the possibility of the preferential excitation of an unpaired target nucleon, two different assumptions are possible. Either the first inter-

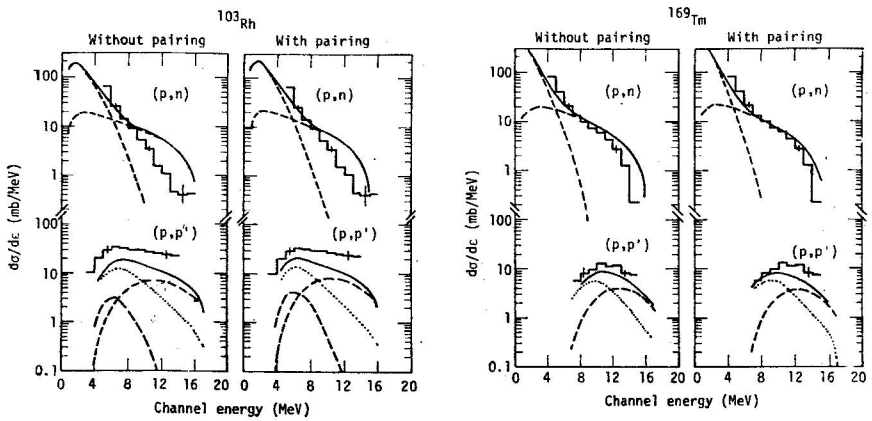

Fig. 16. Comparison of experiment and calculations for reactions induced in ^{103}Rh and ^{169}Tm by 18 MeV protons. The bar graphs show the experimental results; the solid curves show the calculated spectra for a $2p-1h$ initial configuration; the dashed curves show the calculated $T_<$ preequilibrium (hard) and equilibrium (soft) components; the dotted lines show the $T_>$ preequilibrium component (from [37]).

action is with the unpaired nucleon so that the initial configuration is of the $2p - 0h$ type or, as assumed by Griffin and Lee [1, 37], there is simultaneous excitation of the unpaired nucleon during the first particle-hole pair creation interaction, thus forming a $3p - 1h$ state. Figure 17 shows that neither of the interpretations can consistently account for the data. The $2p - 0h$ configuration does reasonably well for the three odd proton targets, although it significantly over-corrects the neutron intensities for the ^{159}Tb and ^{169}Tm targets, while assuming a $3p - 1h$ initial configuration produces quite good agreement for the ^{105}Pd(p, n) results. Figure 18 shows the agreement between calculation and experiment which can be obtained by varying the assumptions made about the role of the unpaired target nucleon separately for each reaction system.

The conclusion which seems to emerge from this analysis is that there is marginal evidence for the utility of substracting the approprate pairing energies of the systems. Assuming initial configurations which assign a special role to the unpaired target nucleons can also produce somewhat improved agreement for some systems relative to the usual $2p - 1h$ assumption. However, no systematic assumption has been found that will produce improved agreement for all odd-A targets. This does not mean, that such an assumption does not exist. It is not impossible that the Coulomb force may play a role in exciting an odd proton with a proton projectile. There may be a dependence

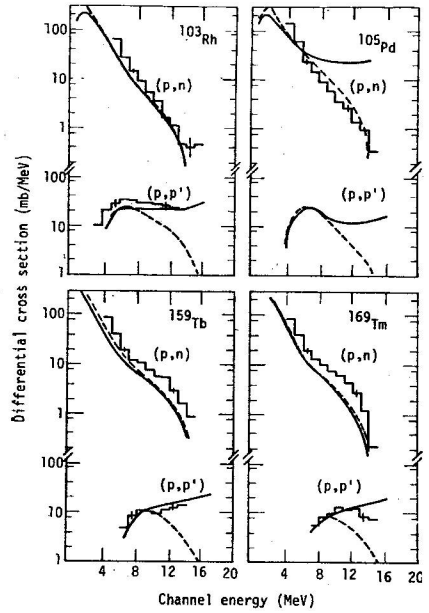

Fig. 17. Comparison of experiment and calculation. The bar graphs show the experimental results, the solid and dashed curves show the calculated spectra for $2p-0h$ and $3p-1h$ initial configurations, respectively. All calculations include a pairing energy correction (from [37]).

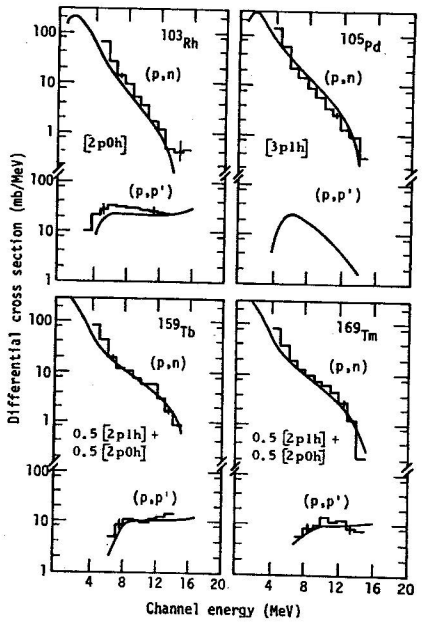

Fig. 18. Comparison of experiment and calculation. The bar graphs show the experimental results while the solid curves show the calculated curves for the indicated initial configurations. All calculations include a pairing energy shift (from [37]).

of the excitation probability of an unpaired nucleon on the pairing energies and thus on the mass number. There may be a dependence on the angular momentum of single particle state of the unpaired nucleon and thus on the amount of surface peaking of its wave function. Nuclear deformation may play a role. All this is pure speculation. To settle the question of the importance of pairing effects in the first phases of a nucleon induced reaction, we need more data of the type shown in Fig. 18. Further, we need data for neutron as well as proton induced reactions to better enable us to discover the systematics of the results, if there are any.

V. SUMMARY AND CONCLUSIONS

It may seem that in choosing to end with a discussion of problems that remain to be solved, I am taking a somewhat negative attitude. I feel that

just the opposite is the case. The Griffin model, like the other models discussed in Sect. II, has now developed to a point where we have confidence in it to correctly estimate the overall magnitudes and spectral shapes for a variety of nuclear reaction systems without the aid of adjustable parameters. The questions which are now being considered are, within the framework of the model, largely second order effects, and the fact that we can even begin to worry about them expresses a certain confidence in the model. Their solution will provide information for future model developments and will also tell us something about nuclear structure (be it the role of isospin, pairing or α-clustering). Thus I personally feel that this is a hopeful and exciting period for preequilibrium models in general and the Griffin model in particular.

REFERENCES

[1] Griffin J. J., Phys. Lett. *17* (1966), 478.
[2] West R. W., Phys. Rev. *141* (1966), 1033.
[3] Barashenkov V. S., Bertini H. W., Chen K., Friedlander G., Harp G. D., Iljinov A. S., Miller J. M., Toneev V. D., Nucl. Phys. *A 187* (1972), 531.
[4] Friedlander G., Kennedy J. W., Miller J. M., *Nuclear and Radiochemistry*. 2nd edition John Wiley, New York 1964.
[5] Harp G. D., Miller J. M., Berne B. J., Phys. Rev. *165* (1968), 1166.
[6] Harp G. D., Miller J. M., Phys. Rev. *C 3* (1971), 1847.
[7] Blann M., Phys. Rev. Lett. *21* (1968), 1357.
[8] Williams F. C., Jr., Phys. Lett. *31 B* (1970), 184.
[9] Cline C. K., Blann M., Nucl. Phys. *A 172* (1971), 225.
[10] Cline C. K., Nucl. Phys. *A 193* (1972), 417.
[11] Cline C. K., Nucl. Phys. *A 195* (1972), 353.
[12] Ribanský I., Obložinský P., Betak E., Nucl. Phys. *A 205* (1973), 545.
[13] Obložinský P., Ribanský I., Acta Phys. Slovaca *24* (1974), 103.
[14] Blann M., Phys. Rev. Lett. *27* (1971), 337.
[15] Blann M., Mignerey A., Nucl. Phys. *A 186* (1972), 245.
[16] Blann M., Phys. Rev. Lett. *28* (1972), 757.
[17] Blann M., Nucl. Phys. *A 213* (1973), 570.
[18] Bertrand F. E., Peele R. W., Phys. Rev. *C 8* (1973), 1045.
[19] Verbinsky V. V., Burrus W. R., Phys. Rev. *117* (1969), 171.
[20] Blann M., *Proceedings of the Europhysics Study Conference on Intermediate Processes in Nuclear Reactions*. Ed. Cindro N., Kulisic P., Mayer-Kuckuk T., Springer-Verlag, Berlin 1973.
[21] Gilbert A., Cameron A. G. W., Can. J. Phys. *43* (1965), 1446.
[22] Kalbach-Cline C., Nucl. Phys. *A 210* (1973), 590.
[23] Bragga-Marcazzan G. M., Gadioli-Erba E., Milazzo-Colli L., Sona P. G., Phys. Rev. *C 6* (1972), 1398.
[24] Ribansky I., Oblozinsky P., Phys. Lett. *45 B* (1973), 318.
[25] Fluss M. J., Miller J. M., D'Auria J. M., Dudley N., Foreman B. M., Jr. Kowalski L., Reedy R. C., Phys. Rev. *187* (1969), 1449.

[26] Lu C. C., Huizenga J. R., Stephan J. C., Gorski A. J., Nucl. Phys. *A 164* (1971), 225.
[27] Vaz L. C., Lu C. C., Huizenga J. R., Phys. Rev. *C 5* (1972), 463.
[28] Wiley J., Pacer J. C., Lux C. R., Porile N. T., Nucl. Phys. *A 212* (1972), 1.
[29] Porile N. T., Pacer J. C., Wiley J., Lux C. R., Phys. Rev. *C 9* (1974), 2171.
[30] Kalbach-Cline C., Huizenga J. R., Vonach H. K., Nucl. Phys. *A 222* (1974), 405.
[31] Kalbach C., Grimes S. M., Wong C., *to be published* (preprint available).
[32] Cline C. K., *Ph. D. Thesis*. University of Rochester, 1970, unpublished.
[33] Birattari C., Gadioli E., Grassi-Strini A. M., Strini C., Tagliaferri G., Zetta L., Nucl. Phys. *A 166* (1971), 605.
[34] Grimes S. M., Anderson J. D., Davis J. C., Wong C., Phys. Rev. *C 7* (1973), 343.
[35] Grimes S. M., Anderson J. D., Davis J. C., Wong C., Phys. Rev. *C 8* (1973), 1770.
[36] Chavarier A., Chevarier N., Demeyer A., Hollinger G., Petrosa P., Tran Minh Duc, Phys. Rev. *C 8* (1973), 2155.
[37] Lee E. V., Griffin J. J., Phys. Rev. *C 5* (1972), 1713.

Received September 9th, 1974